VIP Photodynamic Therapy Very Important Paper

Deutsche Ausgabe: DOI: 10.1002/ange.201507800
Internationale Ausgabe: DOI: 10.1002/anie.201507800

Highly Charged Ruthenium(II) Polypyridyl Complexes as Lysosome-Localized Photosensitizers for Two-Photon Photodynamic Therapy

Huaiyi Huang, Bole Yu, Pingyu Zhang, Juanjuan Huang, Yu Chen, Gilles Gasser, Liangnian Ji, and Hui Chao**

Abstract: *Photodynamic therapy (PDT) is a noninvasive medical technique that has received increasing attention over the last years and been applied for the treatment of certain types of cancer. However, the currently clinically used PDT agents have several limitations, such as low water solubility, poor photostability, and limited selectivity towards cancer cells, aside from having very low two-photon cross-sections around 800 nm, which limits their potential use in TP-PDT. To tackle these drawbacks, three highly positively charged ruthenium(II) polypyridyl complexes were synthesized. These complexes selectively localize in the lysosomes, an ideal localization for PDT purposes. One of these complexes showed an impressive phototoxicity index upon irradiation at 800 nm in 3D HeLa multicellular tumor spheroids and thus holds great promise for applications in two-photon photodynamic therapy.*

Photodynamic therapy (PDT) has expanded the range of medical techniques available to treat certain types of cancer, such as lung, bladder, and ophthalmologic cancer, and urinary tumors.[1] PDT treatments rely on the use of a combination of a photosensitizer (PS) and light. Ideally, a PS should be non-toxic in the absence of light but have a high toxicity for cancer cells upon light exposure.[2] Specifically, the excited state of the PS reacts with the ground state of molecular oxygen ($^3O_2$) to generate reactive oxygen species and notably singlet oxygen ($^1O_2$). In PDT, $^1O_2$ is considered as the primary toxic species that can induce cellular organelle or vasculature damage.[3] However, currently available PDT agents are plagued by a number of issues, including a generally poor water solubility and slow clearance from the body, weak photostability, and the necessity for irradiation with a high-energy one-photon (OP) laser beam.[4] To tackle these drawbacks, two-photon PDT (TP-PDT) agents have emerged over recent years as attractive alternatives to the currently approved PSs.[5] Contrary to OP-PDT, TP-PDT uses low-energy near-infrared laser irradiation, which is less damaging to normal cells and allows for reduced photobleaching of the PSs and deeper tissue penetration.[6]

In view of TP-PDT applications, viable PSs must have a high efficiency for two-photon absorption (TPA), a property that is quantified by the two-photon cross-section (σ_2).[7] Readily available PSs (e.g., porphyrin) generally have low σ_2 values (< 20 GM, where $1\ \mathrm{GM} = 10^{-50}\ \mathrm{cm^4\,s\ molecule^{-1}}$). Although these compounds are preferentially taken up by tumors, their two-photon cross-sections are insufficient for adequate clinical efficacy in TP-PDT.[7] Among the different PSs that have been tested for TP-PDT and more generally for PDT, ruthenium(II) polypyridyl complexes were found to be excellent candidates[8] owing to their attractive photophysical properties (i.e., high water solubility, large σ_2, high $^3O_2$ production, long luminescence lifetime, and excellent chemical and photostability). However, a number of other pertinent factors must be considered for the development of practically useful TP-PDT agents. These include cell uptake and localization, a high phototoxicity index (PI) characterized by a low dark toxicity and high light toxicity, and the biodistribution of the PS. For instance, in cells, the PSs can be localized in the mitochondria, the plasma-membrane endoplasmic reticulum, the lysosomes, the Golgi apparatus, or the nucleus.[9] Owing to the influence of the mitochondrial membrane potential, the mitochondrion is a well-known target for lipophilic, charged metal complexes, such as polypyridyl Ru^{II} complexes, that enter cells mostly by passive diffusion.[10]

However, as the mitochondria function as cellular energy houses, it has been pointed out that mitochondrial localization of a PS could result in high dark cytotoxicity.[11] Furthermore, nucleus localization is generally considered to be unfavorable because of the potential for DNA mutation.[12] Therefore, PSs that target cellular organelles other than the mitochondria or the nucleus are in high demand. With all these requirements in mind, we envisaged preparing highly charged Ru^{II} polypyridyl complexes that do not localize either in the mitochondria or in the nucleus. Herein, we present the synthesis, characterization, and in-depth biological investigation of three highly positively charged homoleptic Ru^{II} complexes (Figure 1) as lysosome-targeting TP-PDT agents. This study demonstrates that such complexes have a great potential in TP-PDT. To the best of our knowledge, this is the first report of a Ru^{II} complex suitable as a lysosome-targeting TP-PDT agent.

In particular, the $[Ru(bpy)_3]^{2+}$ core structure was chosen as octupolar tris(bipyridyl) Ru^{II} complexes have been shown to exhibit excellent TPA properties.[13] In this work, tertiary ammonium groups were added to the core structure to allow

[*] H. Huang,[+] Dr. B. Yu,[+] Dr. P. Zhang, J. Huang, Dr. Y. Chen, Prof. L. Ji, Prof. Dr. H. Chao
MOE Key Laboratory of Bioinorganic and Synthetic Chemistry
School of Chemistry and Chemical Engineering
Sun Yat-Sen University
Guangzhou, 510275 (China)
E-mail: ceschh@mail.sysu.edu.cn
H. Huang,[+] Prof. Dr. G. Gasser
Department of Chemistry, University of Zurich
Winterthurerstrasse 190, CH-8057, Zurich (Switzerland)
E-mail: gilles.gasser@chem.uzh.ch
[+] These authors contributed equally to this work.

Supporting information for this article is available on the WWW under http://dx.doi.org/10.1002/anie.201507800.

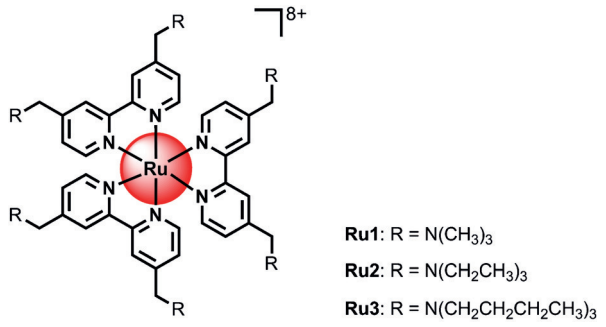

Figure 1. Chemical structures of **Ru1**–**Ru3** (isolated as the perchlorate salts).

for better water solubility as well as to increase the binding affinity of the complexes **Ru1**–**Ru3** to the negatively charged cell membranes. This should facilitate internalization as cells are known to absorb large polar molecules that are unable to passively diffuse through the membrane through an engulfing mechanism. Details on the synthesis and characterization of the Ru^{II} complexes used in this study are included in the Supporting Information (Figures S1–S6). Please note that during the writing of this publication, the synthesis and characterization of **Ru1** was reported by Meyer et al. for use in dye-sensitized solar cells.[14] In this work, as described in the Supporting Information, we used another synthetic route to prepare **Ru1**. Furthermore, crystal data of **Ru2** (Figure S7) are presented in Tables S1 and S2. The photophysical and photochemical properties of the Ru^{II} complexes at room temperature are presented in Figure S8 a. As expected, **Ru1**–**Ru3** exhibit metal-to-ligand charge-transfer (MLCT) absorption bands similar to $[Ru(bpy)_3]^{2+}$, and luminesce around 600 nm. A large Stokes shift for **Ru1**–**Ru3** (150 nm) implies minimal interference between the excitation and scattered light. **Ru1**–**Ru3** have a higher luminescence quantum yield than $[Ru(bpy)_3]^{2+}$ (Table S3). The luminescence lifetimes of **Ru1**–**Ru3** were found to be around 800 ns. Thus, the introduction of the tertiary ammonium groups not only increased the water solubility but also improved the luminescence properties of the Ru^{II} complexes.

The TPA cross-section (σ_2) of **Ru1**–**Ru3** from 700 to 900 nm is shown in Figure S9 and compared to that of $[Ru(bpy)_3]^{2+}$. The largest TPA cross-section of **Ru1**–**Ru3** was found to be around 800 nm with σ_2 values between 185 and 250 GM whereas the σ_2 value of $[Ru(bpy)_3]^{2+}$ was found to be 66 GM under similar conditions. These values are comparable to those of other Ru^{II} complexes previously used for mitochondria-targeting TP-PDT and some octupolar tris(bipyridyl) Ru^{II} complexes (62–180 GM).[15] These TPA values are much higher than that of the clinical photosensitizer H_2TPP (2.2 GM at 800 nm excitation, TPP = tetraphenylporphyrin).[16]

To address the issue of chemical stability, all complexes were exposed to continuous light irradiation and found to exhibit excellent photostability (Figure S8 b). To assess the stability of our coordinatively saturated Ru^{II} complexes in biological media, we performed stability studies in bovine plasma following a recently reported procedure.[17] As clearly evident from the HPLC-UV traces (Figure S10), **Ru1**–**Ru3** showed no apparent decomposition in plasma after three days. Another important parameter for a PDT PS is its ability to produce toxic $^1O_2$. Upon irradiation at 450 nm and by direct comparison with the $^1O_2$ emission areas of phenalenone around 1270 nm, the $^1O_2$ generation quantum yields (Φ_Δ) of **Ru1**–**Ru3** were determined to be 92–99 % in methanol and 49–67 % in D_2O (Figure S8 c). These values are higher than those of $[Ru(bpy)_3]^{2+}$ (Table S3).[18] Furthermore, the Φ values of **Ru1**–**Ru3** were also measured by an indirect method.[19] When 1,3-diphenylisobenzofuran (DPBF) was subjected to these Ru complexes, the emission intensity of DPBF decreased with prolonged irradiation times, indicating the degradation of DPBF by $^1O_2$ (Figure S8 d). The data agreed well with the direct measurements (Table S3).

Electron spin resonance (ESR) spectroscopy was then used to confirm the type of ROS generated by **Ru1**–**Ru3**. 2,2,6,6-Tetramethylpiperidine (TEMP) and 5,5-dimethyl-1-pyrroline *N*-oxide (DMPO) were used as $^1O_2$ (Figure S8 e and Figure S11) and $OH^{\cdot}$ (Figure S8 f) trappers.[20] Characteristic $^1O_2$-induced signals were observed in the ESR spectra under 450 nm light irradiation. The intensity increased with the irradiation time. No radical ion signals could be detected.

We then assessed the lipophilicity/hydrophilicity of **Ru1**–**Ru3** by determining their octanol/water partition coefficient ($\log P_{o/w}$). Such a coefficient is known to allow for predictions of the cell uptake efficiency.[21] **Ru1** (−3.54) and **Ru2** (−3.05) were found to be extremely hydrophilic owing to their positive charge (+8). The core structure $[Ru(bpy)_3]^{2+}$ (−2.52)[21] was found to be slightly less hydrophilic than **Ru1** and **Ru2. Ru3** (−1.55) was the most lipophilic compound of the series owing to its *N*-butyl chains. These values can be easily correlated by visual inspection through observing the luminescence of the octanol/water mixtures containing Ru^{II} complexes (Figure S12). After confirming that **Ru1**–**Ru3** can efficiently produce $^1O_2$ upon light irradiation and that they are stable in biological media, we investigated their cellular uptake pathway and cellular localization. The cellular localization of **Ru1**–**Ru3** was investigated by confocal laser scanning microscopy (CLSM) on cervical cancer HeLa cells as well as HeLa multicellular tumor spheroids (MCTSs). MCTSs are heterogeneous cellular aggregates that are considered as a valid in vitro 3D model to study tissue penetration.[22] As shown in Figure 2 a, **Ru1** showed strong spot-like red luminescence within cells under OP and TP excitation. The TP signal of **Ru1** exhibited significantly deeper penetration into the MCTSs than the OP luminescence signal (Figure 2 b and Figure S13).

The specific cellular target of **Ru1** was further confirmed by colocalization assays. As shown in Figure 2 d, the signal of **Ru1** overlapped well with the commercial lysosome dye LysoTracker Green (LTG). In contrast, using the mitochondrion dye MitoTracker Green (MTG; Figure 2 c) or the nuclear dye Hoechst 33342, a poor correlation coefficient was found (Figure 2 e). **Ru2** and **Ru3** were also found to localize in the lysosomes (Figures S14–S16). Lysosomes function as the waste disposal center within the cell by digesting materials both from outside and inside the cell. There are more than 50 different enzymes inside lysosomes that are capable of breaking down virtually all kinds of biomolecules, including

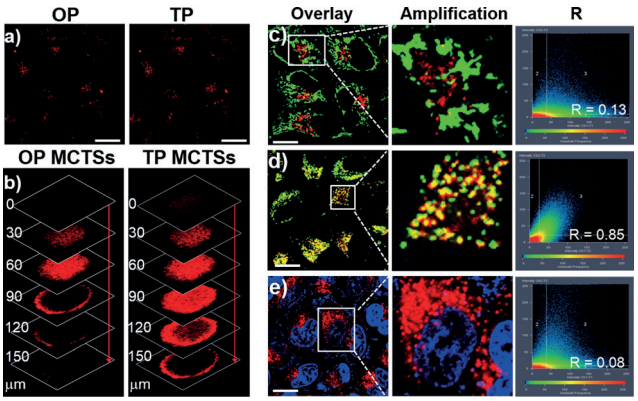

Figure 2. a) OP and TP luminescence images of **Ru1** in a HeLa cell monolayer. b) OP and TP luminescence images of **Ru1** in HeLa MCTSs. c) Colocalization images of **Ru1** and MTG. d) Colocalization images of **Ru1** and LTG. e) Colocalization images of **Ru1** and Hoechst 33342. Scale bar: 30 μm.

proteins, nucleic acids, carbohydrates, lipids, and cellular debris.[23,11] During the endocytosis process, the cell membrane engulfs portions of the external medium forming endosomes, which finally reach the lysosomes.[23,11] Hence, **Ru1**–**Ru3** may enter cells by endocytosis and then localize in lysosomes. Furthermore, we used ICP-MS to quantify the ruthenium uptake by HeLa cells as well as to confirm the cellular localization of **Ru1**–**Ru3** (Figure S17). Most of the Ru^{II} complexes localize in the lysosome rather than in the nucleus. The cellular uptake of **Ru3** was slightly higher than for **Ru1** and **Ru2**. The same trend had been observed during the $\log P_{o/w}$ experiments. As for the cytoplasm fraction, the concentration of ruthenium found in the lysosomes was significantly higher than that in the mitochondria. This finding supports the endocytosis uptake pathway. Further cell uptake mechanism assays in the presence of various inhibitors or under different experimental conditions also confirmed that **Ru1**–**Ru3** are taken up by cancer cells mostly by an energy-dependent endocytosis pathway (Figure S18).

The toxicity of **Ru1**–**Ru3** on HeLa cells was then investigated to assess whether the compounds were toxic in the dark. All complexes were found to be strongly non-toxic towards these cells in the absence of light ($IC_{50} > 300$ μM; Table S4). This observation is extremely encouraging as non-toxicity in the dark is an important property for a PDT agent. The higher dark cytotoxicity of **Ru3** compared to **Ru1** and **Ru2** could be explained by its higher cellular uptake efficiency (see the ICP-MS measurements above). We then investigated the phototoxicity of the Ru^{II} complexes in HeLa cells. For OP-PDT (450 nm, 10 J cm^{-2}), **Ru1** became highly toxic to HeLa cells with an IC_{50} value as low as 1.5 μM (PI = 313). Importantly, untreated cells were also exposed to the same irradiation procedure and found not to be affected. Under similar experimental conditions, the clinically approved PDT agent 5-aminolevulinic acid (5-ALA) displayed a lower phototoxicity and a lower PI than the Ru^{II} complexes studied in this work.

Traditional in vitro PDT drug screening is mainly performed on cell monolayers. However, this kind of cell model presents significant limitations in reproducing the hypoxic conditions and pathophysiology of solid tumors in vivo. Moreover, the multicellular resistance (MCR) that is widely present in solid tumors is not found in cell monolayers.[17] Therefore, MCTSs were employed to further assess the potential of our Ru^{II} complexes. None of the Ru^{II} complexes exhibited dark cytotoxicity towards MCTSs (Table S4). The PI values for MCTSs irradiated at 800 nm (10 J cm^{-2}) were significantly larger than those irradiated by 450 nm light (Table S4). Despite their higher cell uptake, **Ru2** and **Ru3** were found to be less efficient than **Ru1** towards MCTSs. This observation can be attributed to the lower $^1O_2$ generation ability of **Ru2** and **Ru3** compared to **Ru1**. As **Ru1** was found to be the most promising compound of the series, we performed further biological testing with this complex.

Staining of HeLa cells with calcein AM allowed for visualization of the cell viability.[24] Micrographs (Figure S19) showed that cell death was limited to the region irradiated. The ROS generation ability of **Ru1** within cancer cells was then investigated by tracking the morphology changes of HeLa cells by CLSM. In the presence of endogenously generated ROS, the ROS indicator 2,7-dichlorofluorescein diacetate (DCFH-DA) is oxidized to release the green fluorophore DCF. The TP laser beam used was safe for the cells as cell survival was not altered by light exposure (Figure S20). Under TP light irradiation, the morphology of cells pretreated with **Ru1** changed significantly. This included cell shrinkage and the formation of numerous blebs (Figure 3). Meanwhile, the green signal that is due to cellular ROS increased significantly and overlapped well with the red signal of **Ru1**, suggesting sufficient $^1O_2$ generation within cells upon light irradiation. The cellular localization of **Ru1** changed from the lysosomes (Figure 3a) to the cytoplasm (Figure 3b) upon light irradiation, and then, as the irradiation time was extended, to the nucleus and nucleoli (Figure 3c). Similar results have been reported for a porphyrin Ru^{II} complex.[25] Finally, we analyzed the change in the morphology of the cancer cells after TP treatment. For untreated cells (Figure S21a) in the dark and untreated cells after exposure to light (Figure S21b) and cells incubated with **Ru1**–**Ru3** in the dark (Figure S21d), significant morphology changes were not observed, suggesting that the experimental conditions

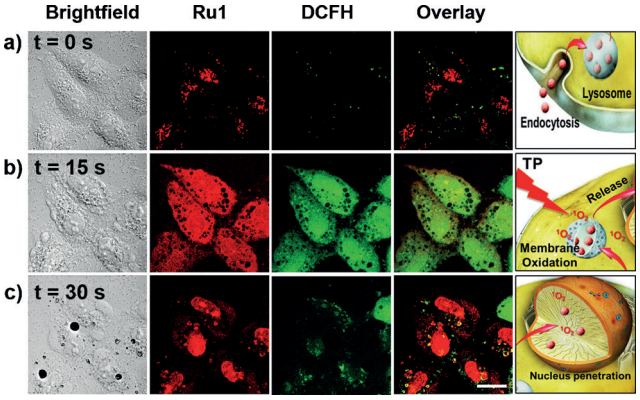

Figure 3. Micrographs of and ROS generation in HeLa cells incubated with **Ru1** (2.0 μM) after irradiation with a two-photon confocal laser (800 nm) for different periods of time. a) $t = 0$ s; b) $t = 15$ s; c) $t = 30$ s. Scale bar: 15 μm.

used were safe towards the cells. However, after irradiation, the morphology of the cells incubated with **Ru1**–**Ru3** changed dramatically (Figure S21 e). The cytosolic constituents of cells spilled into the extracellular space through the damaged plasma membrane in a process that sharply differs from the cell apoptosis induced by cisplatin (Figure S21 c). The nucleus dye SYTOX Green[26] was used to visually clarify cell death by **Ru1**–**Ru3** after light irradiation. Its green fluorescence increases by a factor of 100 when it binds to DNA in late apoptosis or necrotic cells (Figure S22). The significant increase in the green luminescence intensity was only observed in the cells after irradiation. The cells incubated in the dark with **Ru1**–**Ru3** did not die at all. Thus, **Ru1**–**Ru3** caused high cellular oxidative stress after light irradiation and finally induced cell death by necrosis.

In summary, we have prepared highly charged ruthenium-(II) polypyridyl complexes that can specifically accumulate in lysosomes through endocytosis. **Ru1**–**Ru3** have a high water solubility, impressive $^1O_2$ production quantum yields, excellent photostability, marked TP properties, and a low dark cytotoxicity. Importantly, those complexes induce cell necrocytosis upon two-photon irradiation with impressive phototoxicity indexes. We strongly believe that these complexes, especially **Ru1**, hold great promise in two-photon photodynamic therapy.

Acknowledgements

This work was supported by the 973 Program (2015CB856301), the National Science Foundation of China (21172273, 21171177, 21471164, and J1103305), the Program for Changjiang Scholars and Innovative Research Team at the University of China (IRT1298), the Swiss National Science Foundation (SNSF Professorships PP00P2_133568 and PP00P2_157545 to G.G.) and the University of Zurich. We thank Dr. Phuc Ung for helpful discussions. H.H. acknowledges financial support from the China Scholarships Council (201506380026).

Keywords: cancer therapy · lysosomes · photodynamic therapy · ruthenium · singlet oxygen

How to cite: *Angew. Chem. Int. Ed.* **2015**, *54*, 14049–14052
Angew. Chem. **2015**, *127*, 14255–14258

[1] D. E. J. G. J. Dolmans, D. Fukumura, R. K. Jain, *Nat. Rev. Cancer* **2003**, *3*, 380–387.
[2] A. Frei, R. Rubbiani, S. Tubafard, O. Blacque, P. Anstaett, A. Felgentrager, T. Maisch, L. Spiccia, G. Gasser, *J. Med. Chem.* **2014**, *57*, 7280–7292.
[3] A. Naik, R. Rubbiani, G. Gasser, B. Spingler, *Angew. Chem. Int. Ed.* **2014**, *53*, 6938–6941; *Angew. Chem.* **2014**, *126*, 7178–7182.
[4] J. C. Ge, M. H. Lan, B. J. Zhou, W. M. Liu, L. Guo, H. Wang, Q. Y. Jia, G. L. Niu, X. Huang, H. Y. Zhou, X. M. Meng, P. F. Wang, C. S. Lee, W. J. Zhang, X. D. Han, *Nat. Commun.* **2014**, *5*, 4596.
[5] a) A. V. Kachynski, A. Pliss, A. N. Kuzmin, T. Y. Ohulchanskyy, A. Baev, J. Qu, P. N. Prasad, *Nat. Photonics* **2014**, *8*, 455–461; b) T. Gallavardin, C. Armagnat, O. Maury, P. L. Baldeck, M. Lindgren, C. Monnereau, C. Andraud, *Chem. Commun.* **2012**, *48*, 1689–1691.
[6] a) C. S. Lim, G. Masanta, H. J. Kim, J. H. Han, H. M. Kim, B. R. Cho, *J. Am. Chem. Soc.* **2011**, *133*, 11132–11135; b) H. Ke, H. Wang, W. Wong, N. Mak, D. W. J. Kwong, K. Wong, H. Tam, *Chem. Commun.* **2010**, *46*, 6678–6680.
[7] a) M. A. Albota, C. Xu, W. W. Webb, *Appl. Opt.* **1998**, *37*, 7352–7356; b) A. Karotki, M. Khurana, J. R. Lepock, B. C. Wilson, *Photochem. Photobiol.* **2006**, *82*, 443–452.
[8] a) C. Mari, V. Pierroz, S. Ferrari, G. Gasser, *Chem. Sci.* **2015**, *6*, 2660–2686; b) J. D. Knoll, C. Turro, *Coord. Chem. Rev.* **2015**, *282–283*, 110–126; c) R. Lincoln, L. Kohler, S. Monro, H. Yin, M. Stephenson, R. Zong, A. Chouai, C. Dorsey, R. Hennigar, R. P. Thummel, S. A. McFarland, *J. Am. Chem. Soc.* **2013**, *135*, 17161–17175; d) T. Joshi, V. Pierroz, C. Mari, L. Gemperle, S. Ferrari, G. Gasser, *Angew. Chem. Int. Ed.* **2014**, *53*, 2960–2963; *Angew. Chem.* **2014**, *126*, 3004–3007; e) F. Barragán, P. López-Senın, L. Salassa, S. Betanzos-Lara, A. Habtemariam, V. Moreno, P. J. Sadler, V. Marchán, *J. Am. Chem. Soc.* **2011**, *133*, 14098–14108.
[9] C. Mari, V. Pierroz, R. Rubbiani, M. Patra, J. Hess, B. Spingler, L. Oehninger, J. Schur, I. Ott, L. Salassa, S. Ferrari, G. Gasser, *Chem. Eur. J.* **2014**, *20*, 14421–14436.
[10] A. C. Komor, J. K. Barton, *Chem. Commun.* **2013**, *49*, 3617–3630.
[11] M. Dickerson, Y. Sun, B. Howerton, E. C. Glazer, *Inorg. Chem.* **2014**, *53*, 10370–10377.
[12] J. Bertram, *Mol. Aspects Med.* **2000**, *21*, 167–223.
[13] a) B. J. Coe, *Coord. Chem. Rev.* **2013**, *257*, 1438–1458; b) B. J. Coe, J. A. Harris, B. S. Brunschwig, I. Asselberghs, K. Clays, J. Garín, J. Orduna, *J. Am. Chem. Soc.* **2005**, *127*, 13399–13410.
[14] W. B. Swords, G. C. Li, G. J. Meyer, *Inorg. Chem.* **2015**, *54*, 4512–4519.
[15] a) S. C. Boca, M. Four, A. Bonne, B. van der Sanden, S. Astilean, P. L. Baldeck, G. Lemercier, *Chem. Commun.* **2009**, 4590–4592; b) F. N. Castellano, H. Malak, I. Gryczynski, J. R. Lakowicz, *Inorg. Chem.* **1997**, *36*, 5548–5551.
[16] T. Ishi-i, Y. Taguri, S. I. Kato, M. Shigeiwa, H. Gorohmaru, S. Maeda, S. Mataka, *J. Mater. Chem.* **2007**, *17*, 3341–3346.
[17] a) H. Huang, P. Zhang, H. Chen, L. Ji, H. Chao, *Chem. Eur. J.* **2015**, *21*, 715–725; b) H. Huang, P. Zhang, B. Yu, Y. Chen, L. Ji, H. Chao, *J. Med. Chem.* **2014**, *57*, 8971–8983; c) H. Huang, P. Zhang, Y. Chen, L. Ji, H. Chao, *Dalton Trans.* **2015**, *44*, 15602–15610; d) P. Zhang, H. Huang, Y. Chen, J. Wang, L. Ji, H. Chao, *Biomaterials* **2015**, *53*, 522–531.
[18] D. Garcìa-Fresnadillo, Y. Georgiadou, G. Orellana, A. Buraun, E. Oliveros, *Helv. Chim. Acta* **2004**, *79*, 1222–1228.
[19] J. Park, D. W. Feng, S. Yuan, H. C. Zhou, *Angew. Chem. Int. Ed.* **2015**, *54*, 430–435; *Angew. Chem.* **2015**, *127*, 440–445.
[20] B. J. Jiang, L. F. Hu, X. C. Shen, S. C. Ji, Z. J. Shi, C. J. Liu, L. Zhang, H. Liang, *ACS Appl. Mater. Interfaces* **2014**, *6*, 18008–18017.
[21] C. A. Puckett, J. K. Barton, *J. Am. Chem. Soc.* **2007**, *129*, 46–47.
[22] T. T. Goodman, C. P. Ng, S. H. Pun, *Bioconjugate Chem.* **2008**, *19*, 1951–1959.
[23] a) C. Settembre, A. Fraldi, D. L. Medina, A. Ballabio, *Nat. Rev. Mol. Cell Biol.* **2013**, *14*, 283–296; b) C. B. He, Y. P. Hua, L. C. Yin, C. Tang, C. H. Yin, *Biomaterials* **2010**, *31*, 3657–3666.
[24] A. A. Holder, D. F. Zigler, M. T. Tarrago-Trani, B. Storrie, K. J. Brewer, *Inorg. Chem.* **2007**, *46*, 4760–4762.
[25] J. X. Zhang, J. W. Zhou, C. F. Chan, T. C. Lau, D. W. Kwong, H. L. Tam, N. K. Mak, K. L. Wong, W. K. Wong, *Bioconjugate Chem.* **2012**, *23*, 1623–1638.
[26] I. Johnson, M. T. Z. Spence, *The Molecular Probes Handbook*, *A Guide to Fluorescent Probes and Labeling Technologies*, *11th ed.*, Molecular Probes, Eugene, **2010**.

Received: September 7, 2015
Published online: October 8, 2015

